

Sensor Fusion for Airborne Landmine Detection

Miranda A. Schatten

U.S. Army Research, Development and Engineering Command, Communications Electronics
Research Development and Engineering Center, Night Vision and Electronic Sensors Directorate
(RDECOM CERDEC NVESD)
Ft. Belvoir, VA 22060

Paul D. Gader, Jeremy Bolton, Alina Zare, Andres Mendez-Vasquez

[†]Department of Computer and Information Science and Engineering
University of Florida
Gainesville, FL 32611-6120

ABSTRACT

Sensor fusion has become a vital research area for mine detection because of the countermining community's conclusion that no single sensor is capable of detecting mines at the necessary detection and false alarm rates over a wide variety of operating conditions. The U. S. Army Night Vision and Electronic Sensors Directorate (NVESD) evaluates sensors and algorithms for use in a multi-sensor multi-platform airborne detection modality. A large dataset of hyperspectral and radar imagery exists from the four major data collections performed at U. S. Army temperate and arid testing facilities in Autumn 2002, Spring 2003, Summer 2004, and Summer 2005. There are a number of algorithm developers working on single-sensor algorithms in order to optimize feature and classifier selection for that sensor type. However, a given sensor/algorithm system has an absolute limitation based on the physical phenomena that system is capable of sensing. Therefore, we perform decision-level fusion of the outputs from single-channel algorithms and we choose to combine systems whose information is complementary across operating conditions. That way, the final fused system will be robust to a variety of conditions, which is a critical property of a countermining detection system.

In this paper, we present the analysis of fusion algorithms on data from a sensor suite consisting of high frequency radar imagery combined with hyperspectral long-wave infrared sensor imagery. The main type of fusion being considered is Choquet integral fusion. We evaluate performance achieved using the Choquet integral method for sensor fusion versus Boolean and soft "and," "or," mean, or majority voting.

Keywords: sensor fusion, landmines, hyperspectral, Choquet, countermining

1. INTRODUCTION

In the last few years, the U. S. Army Night Vision and Electronic Sensors Directorate (NVESD) has been conducting an evaluation of sensors and processing techniques for a fusion solution to airborne minefield detection. Sensor fusion is used to exploit the different physics to which each sensor modality responds. This can be done for several reasons: to provide confirmation for a detection, to decimate detections that one sensor can identify as false alarms, to provide a more robust system when each sensor works best in different conditions, or to concatenate detections when each sensor responds to a different type of target. It is the latter two cases which we address in this paper, in which we exploit the complementary nature of radar and infrared sensors. For example, long-wave infrared sensors perform well in detecting buried mines in dry sandy soil, while RF sensors perform poorly. It has been shown that high-frequency SARs such as the Lynx Ku-band SAR¹ has some detection capability over surface targets only, while long-wave infrared (LWIR) hyperspectral imaging (HSI) sensors such as AHI² performs well against buried mines. While a simple "OR" fusion would capture detections from both sensors, it would also concatenate every false alarm picked up by each sensor, resulting in a very high false alarm rate. On the other hand, simple "AND" fusion would not take into account the

complementary nature of the sensors. It is not obvious what the best operator for aggregating information from multiple algorithms operating on multiple sensors. In this work, we strive to implement an adaptive weighting that should be applied to each sensor at every pixel to stress the importance of that sensor's data at that point on the ground. Specifically, a method for mapping multiple mine detector confidence values obtained from multiple algorithms operating on multiple sensors is described. The method is based on Choquet integration. The adaptive weights used in the integration are estimated on training data by minimizing a Minimum Classification Error (MCE) based training algorithm. The weights define adaptive aggregation operators that are used test data.

2. DATASET DESCRIPTION

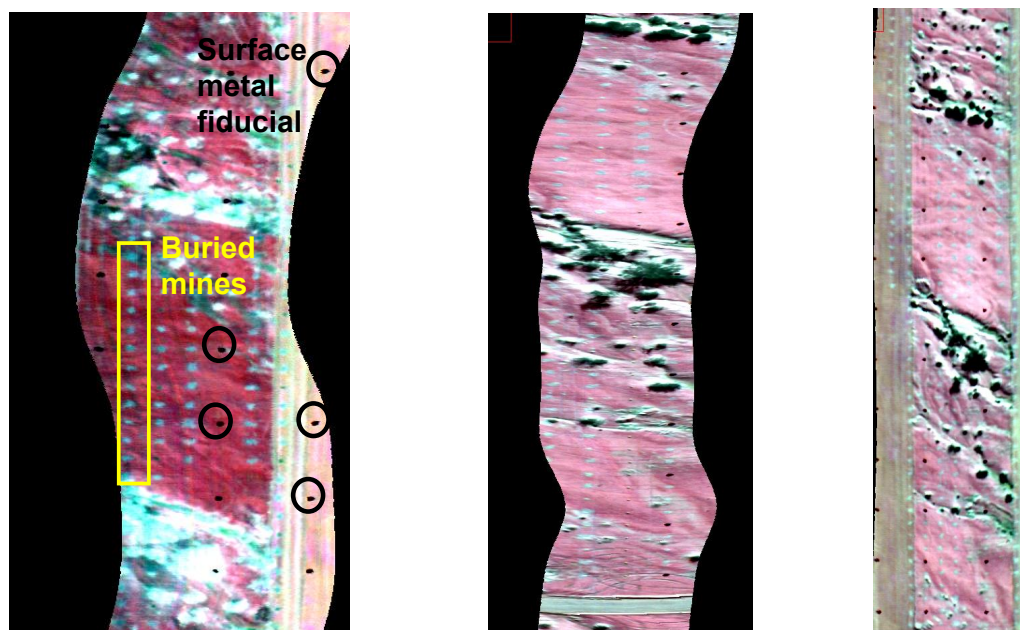
We examined Lynx SAR and AHI HSI data acquired at an NVESD data collection, which took place at an arid testing site in Apr 2003. The Lynx flew in a King Air 200 fixed wing aircraft at altitudes around 8500', and the AHI flew in a Twin Otter fixed-wing aircraft at 1000', and 2000'. The Lynx SAR was VV polarized and deployed in spotlight mode in order to achieve 4" resolution on the ground. The AHI sensor has a 0.5 mRad IFOV and a 150 Hz frame rate, which provides resolutions of 6"x14" at 1000' and 12"x14" at 2,000'. Because the data collection involved multiple airborne sensors, a significant effort was made to collect the data in a methodical and meaningful manner. As such, the landmine targets were placed in a grid with 5 m spacing, and within this area, fiduciary aluminum top hat markers were placed in a grid with 20 m spacing. Locations of both were measured with a differential GPS, and the resulting sensor imagery was subjected to a semi-automated fiducial detection algorithm³ in order to then locate the precise UTM coordinates of each target. Typical errors in ground truthing were less than a target size (1'). Since the Lynx sensor GSD was 4", this excludes the possibility of true pixel-level fusion. Therefore, our focus has been on fusion at the feature- and the decision-level. In this paper, we discuss decision-level fusion.

Imagery from the one site at the data collection were used for fusion. As shown in figure 1, the site contained two types of background clutter over its 360 m x 60 m area. The "lanes," as shown on the left side of the photo, are graded strips which are used as roads and are free of vegetative clutter. The "spaces" consist of the natural desert varnish malapai, and contain washes which support vegetation ranging from the size of a landmine to a 15' palo verde tree or saguaro cactus. Approximately 300 metal and plastic anti-tank landmines were deployed at this site, both on the surface and buried to flush or 4" depths.



Fig 1. Photo of test site at the NVESD data collection at an arid testing location

Coverage of the site required three images from the AHI sensor, and a single image from the Lynx. Figs 2-4 show false color AHI imagery at 1000' AGL over the site. The Red channel of the false color image holds radiance at 8.14 μm which is just before the Reststrahlen peak; the Green channel is set to 8.93 μm at the beginning of the Reststrahlen peak, and Blue is set to 10 μm which is just at the tail end of the peak. With this color scale, disturbed earth (buried mines) appears cyan, malapai appears reddish, and vegetation is white because of its neutral spectrum. Fig 5 shows a Lynx SAR image over the same site.



Figs. 2-4 Airborne AHI imagery over the site; R = 8.14 μm , G = 8.93 μm , B = 10.0 μm

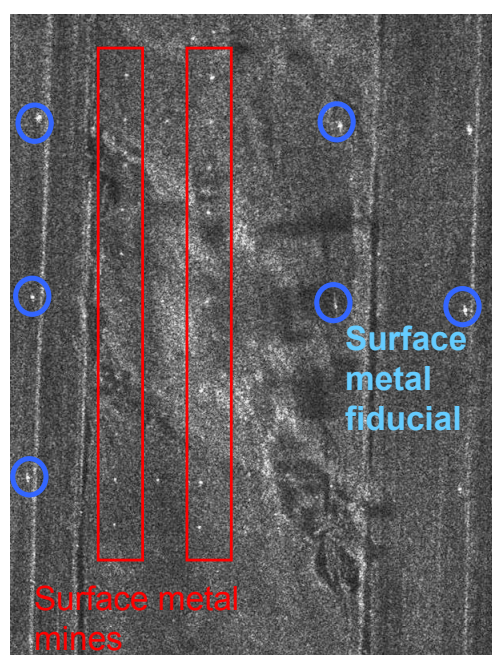


Fig. 5 A Lynx SAR image over the site

3. CHOQUET INTEGRALS AND FUZZY MEASURES

This section defines fuzzy measures and the Choquet integral, and derives the optimization methods for learning the adaptive weighting. First fuzzy measures and then Choquet integrals are defined. Following that, the MCE objective

function is defined. The MCE objective function is minimized via gradient descent. A brief description of the derivatives, which are non-trivial, of the objective function is given. Full details of the derivation can be found in the literature⁴.

Sec. 2.1. Fuzzy Measures

Fuzzy measures are generalizations of classical measures, including probability measures⁵⁻⁸. A fuzzy measure, g , on a finite set $X = \{x_1, \dots, x_N\}$ is a function on the power set of X , $g: 2^X \rightarrow [0,1]$ which satisfies:

- (i) $g(\emptyset) = 0, g(X) = 1$
- (ii) $g(A) \leq g(B)$ if $A \subseteq B$, where $A, B \subseteq X$

Note that g is not necessarily additive but all additive measures are fuzzy measures. In particular, all probability measures are fuzzy measures. The notion of fuzzy measure is very general. In sensor and algorithm fusion, parameters of fuzzy measures must be specified. In general, a fuzzy measure consists of $2^n - 2$ free parameters, one for every subset of X except for the empty set and X itself. Given limited training data, it is often more robust to define special families of fuzzy measures that are characterized by a smaller number of free parameters.

The Sugeno measures are a class of fuzzy measures that have been used for information fusion and that are characterized by only n free parameters^{8,9}. In the research described in this paper, Sugeno measures are used to perform sensor and algorithm fusion. A Sugeno measure, g , on a finite set X is defined for sets $A, B \subseteq X$, with $A \cap B = \emptyset$, by

$$g(A \cup B) = g(A) + g(B) + \lambda g(A)g(B), \quad \text{with } \lambda > -1 \quad (1)$$

When $\lambda = 0$, the Sugeno measure is a probability measure. Let $g_i = g(\{x_i\})$. The values $\{g_1, g_2, \dots, g_n\}$ are called densities. Since $g(X) = 1$, finding λ is equivalent to solving

$$\lambda + 1 = \prod_{i=1}^n (1 + \lambda g_i), \quad \text{where } \lambda \neq 0 \quad (2)$$

It has been shown that there exists a unique solution⁹ $\lambda \in (-1, \infty)$, $\lambda \neq 0$. Thus, the n densities determine the 2^n values of a Sugeno measure. As a matter of notation, it is typical to use g to denote Sugeno measures and μ to denote general measures.

In fusion, X represents a set of detectors. The measure of a set of detectors can be more, less, or the same as the sum of the measures of the detectors. The Choquet integral provides the mathematically based method by which confidence values from the detectors are combined with the measure of the detectors to produce a final confidence for fusion.

Sec. 2.2. Choquet Integrals

A discrete Choquet integral is a nonlinear transformation that integrates a real function with respect to a fuzzy measure. Let f be a function $f: X \rightarrow [0,1]$ which represents the evidence provided by the detectors in X .

To define the discrete Choquet integral, we represent a permutation of the values of h into an increasing sequence using parenthesized subscripts, that is

$$0 = f(x_{(0)}) \leq f(x_{(1)}) \leq f(x_{(2)}) \leq \dots \leq f(x_{(N)}) \leq 1. \quad (3)$$

Let $A_{(i)} = \{x_{(i)}, \dots, x_{(N)}\}$. The discrete Choquet fuzzy integral with respect to a fuzzy measure g is defined by

$$C_g(f) \equiv \sum_{i=1}^n f(x_{(i)})[g(A_{(i)}) - g(A_{(i+1)})] = \sum_{i=1}^n [f(x_{(i)}) - f(x_{(i+1)})]g(A_{(i)}) \quad (4)$$

where $g(A_{(N+1)}) \equiv f(x_{(0)}) \equiv 0$. The equations for $C_g(f)$ appear linear, but sorting makes them nonlinear. Thus, the weight given to a particular algorithm may be different depending on where in the sort the algorithm appears.

The Choquet integral defines different operators for different measures. For example, soft AND and OR operators and voting operators can be defined using measures that depend only on the cardinality of the set argument. A wide variety of operations can be performed.

Sec. 2.3. Minimum Classification Error

In this section, we provide an overview of the MCE training algorithm, which is described in detail in the literature⁴. Some extra notation is needed to make a reference to objects in the classification problem. Let Ω denote the set of objects to be classified. In this particular application, the elements of Ω are subimages of the SAR and Hyperspectral images. Each information source x_i for $i=1, \dots, n$ is a function $x_i: \Omega \rightarrow [0, 1]$. For each $\omega \in \Omega$, we define $f_\omega: X \rightarrow [0, 1]$ by $f_\omega(x_i) = x_i(\omega)$.

In MCE training, we do not consider cost functions that use desired outputs. We instead consider a cost function that depends on a difference between confidences of different classes. These differences are called dissimilarity measures. Note that for correct classification, dissimilarity measures are negative. The dissimilarity measure we use is

$$d_M(f_\omega) = -C_{g_M}(\phi_M[f_\omega]) + C_{g_N}[\phi_N[f_\omega]] \quad \text{and} \quad d_N(f_\omega) = -d_M(f_\omega) \quad (5)$$

where the subscript N and M denote the “Mine” and “Non-mine” classes, respectively. The functions ϕ_M and ϕ_N are functions that map the values of f_ω to confidences that ω represents a mine or does not represent a mine respectively. Here we use,

$$\begin{aligned} \phi_M[f_\omega(x)] &= F_M(x(\omega)) = p_M(y \leq x(\omega)) \\ \phi_N[f_\omega(x)] &= 1 - F_N(x(\omega)) = p_N(y > x(\omega)) \end{aligned} \quad (6)$$

where F_M and F_N are the cumulative distribution functions for confidence values produced by x for mines and non-mines, respectively.

We define the loss functions,

$$l_i(f_\omega) = \begin{cases} \frac{1}{1 + e^{(-cd_i(f_\omega))}} & d_i(f_\omega) > 0 \\ 0 & d_i(f_\omega) \leq 0 \end{cases} \quad i \in \{M, N\} \quad (7)$$

It has the property that correctly classified samples have zero loss. With this loss function (7) and the dissimilarity measure (5), we seek to minimize the following cost function

$$E = \sum_{\omega \in M} l_M(f_\omega) + \sum_{\omega \in N} l_N(f_\omega) \quad (8)$$

We minimize using gradient descent. We therefore need to know the derivatives of E with respect to all the densities. We have that

$$\frac{\partial E}{\partial g_M^j} = \sum_{\omega \in M} l_M(f_\omega)(1-l_M(f_\omega)) \frac{\partial d_M(f_\omega)}{\partial g_M^j} + \sum_{\omega \in N} l_N(f_\omega)(1-l_N(f_\omega)) \frac{\partial d_N(f_\omega)}{\partial g_M^j} \quad (9)$$

where g_i^j represents the j^{th} density for the i^{th} class. Now, the term $\frac{\partial d_k(f_\omega)}{\partial g_i^j}$ is equal to

$$\frac{\partial d_k(f_\omega)}{\partial g_i^j} = \begin{cases} -\frac{\partial C_{g_k}(f_\omega)}{\partial g_i^j} & k = i \\ \frac{\partial C_{g_i}(f_\omega)}{\partial g_i^j} & k \neq i \end{cases} \quad (10)$$

Each of these expressions involves the derivative of the Choquet integral with respect to a density. These derivatives, which are somewhat involved to derive but easy to implement, have been derived in the literature⁴. We provide the formulas without the derivation here for completeness.

We use (4) to compute the partial derivative of $C_g(f)$ with respect to g_j . Note that λ is not independent of g_j because, according to (2), λ changes whenever any density changes. Thus $\frac{\partial \lambda}{\partial g_j} \neq 0$. Also, since $g(A_{(i)})$ is dependent on λ ,

$g(A_{(i)})$ depends on g_j . The only $g(A_{(i)})$ value that may be independent of λ is $g(A_{(n)}) = g(\{x_{(n)}\}) = g_{(n)}$. Thus, the partial derivatives are

$$\frac{\partial C_g(f)}{\partial g_j} = \sum_{i=1}^n f(x_{(i)}) \left(\frac{\partial g(A_{(i)})}{\partial g_j} - \frac{\partial g(A_{(i+1)})}{\partial g_j} \right) \quad (11)$$

To derive $\frac{\partial g(A_{(i)})}{\partial g_j}$ consider that, according to (1), $g(A_{(i)}) = g_{(i)} + g(A_{(i+1)}) + \lambda g_{(i)} g(A_{(i+1)})$. Therefore

$$\frac{\partial g(A_{(i)})}{\partial g_j} = \begin{cases} 1 + \lambda g(A_{(i+1)}) + g_{(i)} g(A_{(i+1)}) \frac{\partial \lambda}{\partial g_j} + (1 + \lambda g_{(i)}) \frac{\partial g(A_{(i+1)})}{\partial g_j}, & \text{if } (i) \neq n, (i) = j \\ (1 + \lambda g_{(i)}) \frac{\partial g(A_{(i+1)})}{\partial g_j} + g_{(i)} g(A_{(i+1)}) \frac{\partial \lambda}{\partial g_j}, & \text{if } (i) \neq n, (i) \neq j \\ 1, & \text{if } (i) = n, j = n \\ 0, & \text{if } (i) = n, j \neq n \end{cases} \quad (12)$$

After a bit of work we obtain

$$\frac{\partial \lambda}{\partial g_j} = \frac{\lambda^2 + \lambda}{(1 + g_j \lambda) \left[(1 - (\lambda + 1) \sum_{i=1}^n \left(\frac{g_i}{1 + g_i \lambda} \right) \right]}, \lambda \neq 0 \quad (13)$$

These equations provide all the information necessary to compute the value of the derivatives of Choquet integrals with respect to densities.

4. Algorithm Description

In the experimental results, Choquet integrals with respect to Sugeno measures were used to perform fusion of detection confidence values from multiple algorithms applied to the the AHI and SAR sensor data. Sugeno measures that optimized the MCE criteria were identified on training sets use the MCE derived, gradient descent algorithm.

Two single-channel algorithms were applied to the AHI data: the TRA Minefield Target Detection (MTD) and the Reed-Xiaoli (RX) algorithm. The MTD is a physics-based algorithm that performs anomaly detection on the hyperspectral endmember which most closely resembles disturbed earth. RX^{10} is a statistically-based algorithm which finds spectral anomalies to the local background. Two algorithms operated on the SAR imagery, the logistic Gaussian reduction function (LGRF) et al^{11,12} and the Random Set (RS) detector¹³. Since they operated on a single sensor which did not yield significant complementary information, the AND of the LGRF and Random Set method was used to produce a single output value for the SAR detector. Thus, two detection statistic outputs from hyperspectral imagery, the MTD and RX algorithms, and one SAR algorithms, the soft AND of LGRF and RS were fused using this Choquet integral technique.

5. Sensor Fusion Detection Results

As described in Section 2, landmine detection experiments were performed using airborne data collected over minefields at an arid test site. The imaging Lynx SAR and the AHI hyperspectral sensor were separately flown over the arid site which contained a variety of surface and buried mines.

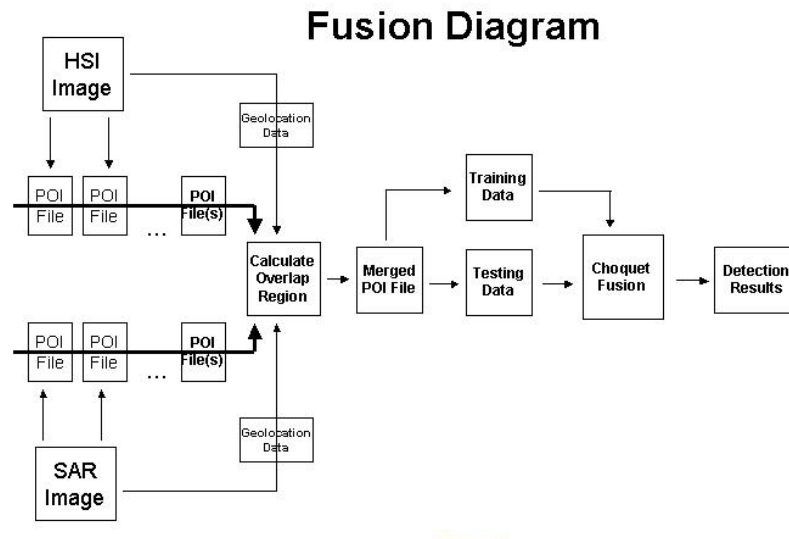


Fig 6. This flow chart illustrates the main steps in the fusion process, beginning with the original imagery and ending with detection results.

Experiments presented here involved 3 HSI images and 3 SAR images that overlapped each of the HSIs. The subsequent 3 overlap regions are areas where the SAR and AHI imagery overlap. Cross validation experiments were performed. In these experiments, for each overlap region optimal Sugeno measures were calculated using all the overlap regions except the given one and then tested on the given one. Testing involves assigning a confidence value to each alarm.

Feature and detector values were then calculated at points of interest (POIs) that were selected by pre-screeners. POIs are points in the image where there is a suspected target determined by a pre-screener. POIs were then merged (grouped) into datasets that were used for training and testing as mentioned above. These feature and detector values are the input to the Choquet integral and the output is a measure of the confidence of detection.

The results are illustrated in ROC curves. A single ROC curve was created for each of the three overlap regions and one was created for all three overlap regions. The ROC curves are shown on a log scale to emphasize the improvement in PD at very low FARs. For each overlap region, the MCE Choquet fusion results are compared to the individual detectors/features and Mean fusion – simply taking the mean of the detectors. They were compared to the Mean operator since it was usually the best competition (i.e. Mean usually outperformed AND / OR operators).

In all the overlap regions, Choquet fusion outperforms generic fusion methods, and outperforms the best individual detectors in each of the overlap regions except one. The Choquet fusion results outperformed the Mean fusion by 10% to 20% PD at bench mark FARs – 0.01 FA/m² and 0.001 FA/m² – in each of the overlap regions. The fusion increased the PD of the best individual detectors by 20% – 30% at these FARs, except at 0.001 FA/m² in the second overlap region.

6. Acknowledgements

The authors are grateful to the many people who contributed to formation and analysis of the WAAMD dataset. Of particular note in this paper are those who created the single-channel algorithms which were used for fusion: Ed Winter at TRA and Lawrence Carin at Duke University. In addition, we'd like to thank Kenny Chamberlin who contributed to the derivation of the Choquet integral. The University of Florida research was partially supported by the Army Research Office and U. S. Army Research Laboratory grant #W911NF-05-1-0067 and was accomplished under Cooperative Agreement Number DAAD19-02-2-0012. The views and conclusions contained in this document are those of the authors and should not be interpreted as representing the official policies, either expressed or implied, of the Army Research Office, Army Research Laboratory, or the U. S. Government. The U. S. Government is authorized to reproduce and distribute reprints for Government purposes notwithstanding any copyright notation hereon. We thank William Clarke and Michael Cathcart for their support of this work.

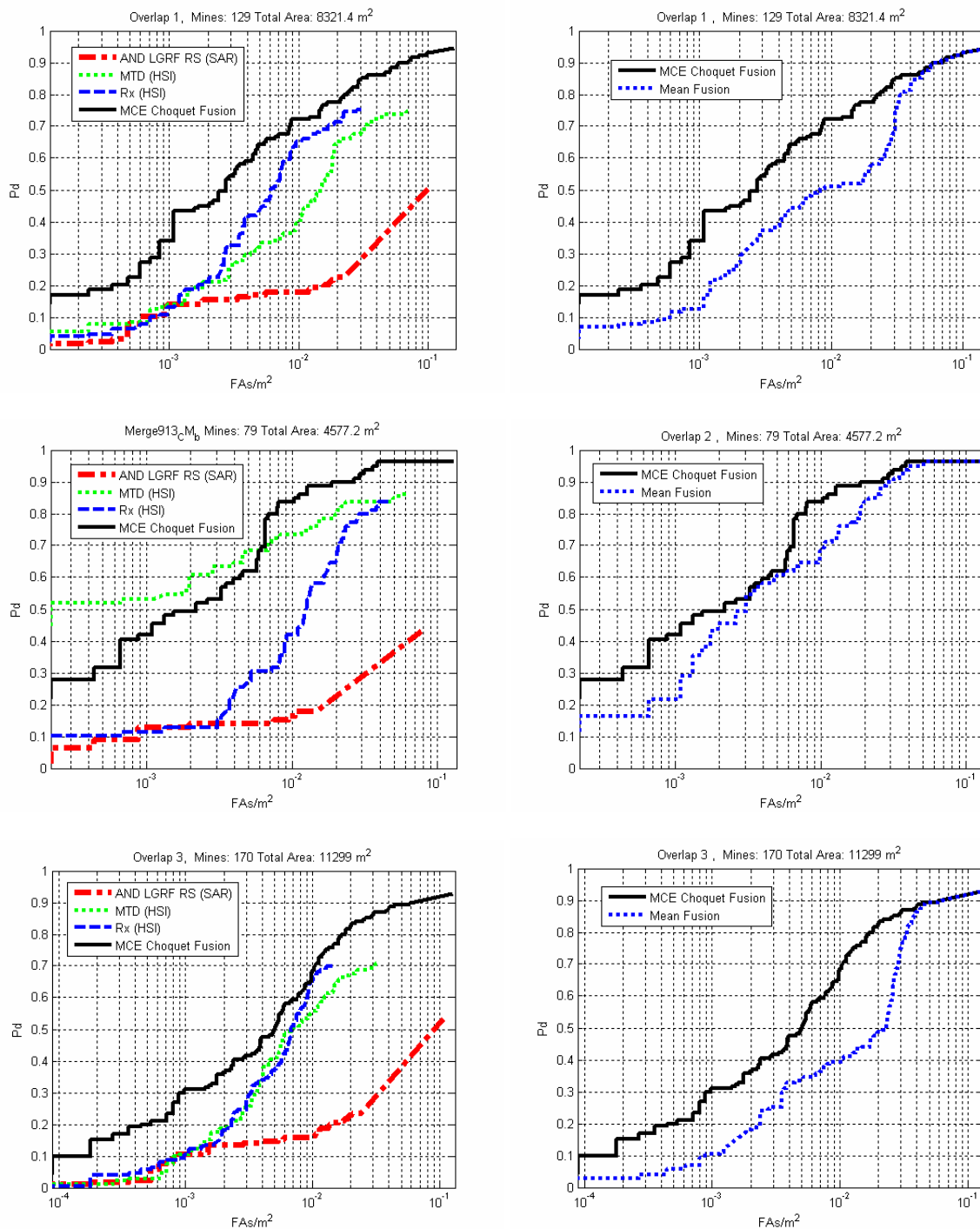


Figure 7. ROC curves for the various overlap regions in the experiment. Each row of the figure corresponds to one overlap region. The first column compares the MCE trained Choquet fusion to the individual detectors. The second column compares the MCE Choquet fusion to mean fusion, which performed better than soft AND, OR, and majority voting.

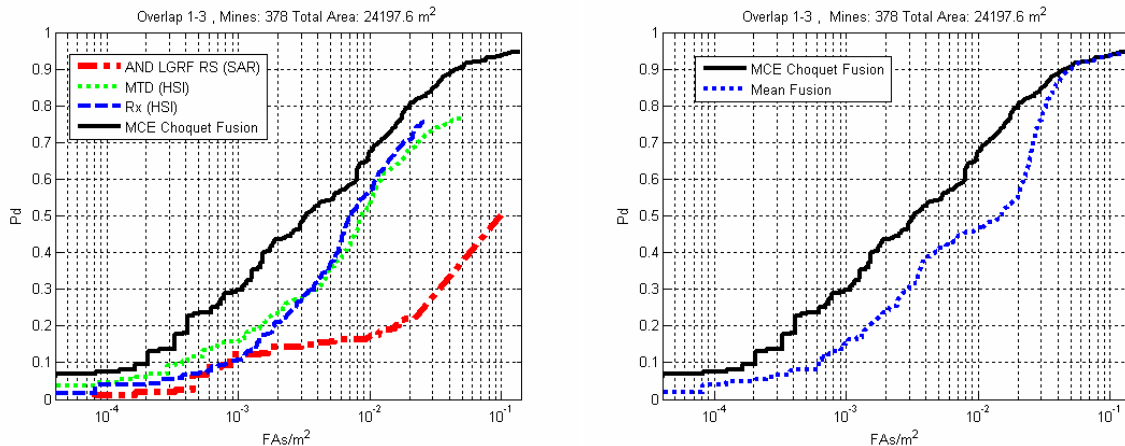


Figure 8. ROC curve combining all overlap regions.

7. References

- [1] S. I. Tsunoda, F. Pace, J. Stence, M. Woodring, "Lynx: A high-resolution synthetic aperture radar", *Proceedings of SPIE Aerosense, SPIE Conference on Radar Sensor Technology*, SPIE Volume 3704, Orlando, Florida, April 1999.
- [2] Lucey, Paul G., Tim Williams, Marc Mignard, Jeffery Julian, Daniel Kokobun, Gregory Allen, David Hampton, William Schaff, Michael Schlangen, Edwin M. Winter, William Kendall, Alan Stocker, Keith Horton, Anu P. Bowman, "AHI: An airborne long wave infrared hyperspectral imager", *Proceedings, SPIE Conference on Airborne Reconnaissance*, pp 36-43, San Diego California, 1998
- [3] William C. Radzelovage, Anthony J. Pawlak, Brian J. Barbour, Erik J. Degraaf and Andrew M. Piper, "An Evaluation Strategy and Co-Registered Imagery Database Supporting Sensor and Algorithm Fusion Studies for Airborne Minefield Detection", *Proceedings of SPIE, SPIE Conference on Detection and Remediation Technologies for Mines and Minelike Targets IX*, SPIE Volume 5415, pp 1118-1129, Orlando, Florida, April 2004.
- [4] Andres Mendez-Vazquez, P. D. Gader, J. M. Keller, K. Chamberlin, "Minimum Classification Error Training for Choquet Integrals with Applications to Landmine Detection", *IEEE Trans. Fuzzy Systems* (submitted).
- [5] M. Grabisch, T. Murofushi, and M. Sugeno, *Fuzzy Measures and Integrals: Theory and Applications*. Studies in Fuzziness and Soft Computing. Physica Verlag, Heidelberg, 2000.
- [6] M. Grabisch, H. T. Hguyen, and E. A. Walker, *Fundamentals of Uncertainty Calculi with Applications to Fuzzy Inference*, Kluwer Academic Publishers, Dordrecht, 1995.
- [7] S. Auephanwirayakul, J. Keller, and P. D. Gader, "Generalized Choquet Fuzzy Integral Fusion", *Information Fusion*, Vol. 3, No. 1, pp. 69-85, March 2002.
- [8] J. M. Keller, P. D. Gader, Hossein Tahani, Jung-Hsien Chiang, and Magdi Mohamed, "Advances in Fuzzy Integration for Pattern Recognition," *Fuzzy Sets and Systems*, Vol. 65, pp. 273-283, 1994.
- [9] H. Tahani and J. Keller, "Information Fusion in Computer Vision using the Fuzzy Integral", *IEEE Trans. Systems, Man, and Cybernetics*, 20(3):733-741, 1990.
- [10] I.S. Reed and X. Yu, "Adaptive Multiple-Band CFAR Detection of an Optical Pattern with Unknown Spectral Distribution," *IEEE Trans on Acoustics, Speech, and Sig. Proc.* **38**(10), 1760-1770 (1990).
- [11] [10] D. Williams, X. Liao, Y. Xue and L. Carin, "Logistic regression classification with incomplete data," *Proc. International Conf. Machine Learning*, 2005.
- [12] X. Liao, Y. Xue and L. Carin, "Logistic regression with an auxiliary data source," *Proc. International Conf. Machine Learning*, 2005.

[13] P. D. Gader, Wen-Hsiung Lee, and Andres Mendez-Vasquez, "Continuous Choquet Integrals with respect to random sets with applications to landmine detection", *Proceedings IEEE Conference Fuzzy Systems*, Budapest, Hungary, July 2004, CDROM.